JOURNAL OF OPTOELECTRONICS AND ADVANCED MATERIALS Vol. 9, No. 5, May 2007, p. 1540 - 1545

# Studies on synthesis and characterization of $Co_3O_4$ powders for CO oxidation

D. BERGER[a,b*], F. MORFIN[b], C. MATEI[a], J. C. VOLTA[b]
[a]*"Politehnica" University of Bucharest, 1 Polizu street, 011061, Bucharest, Romania*
[b]*Institut de Recherches sur la Catalyse, CNRS, 2 avenue Albert Einstein, 69626 Villeurbanne, France*

$Co_3O_4$ nanopowders were synthesised by thermal treatment of different precursors obtained by precipitation at constant pH value using cobalt nitrate or sulphate as cobalt salt and ammonia or potassium hydroxide as precipitating agent. The effect of different parameters as reaction and calcination temperature, type of precipitating agent and cobalt salt on $Co_3O_4$ crystallite size and specific surface area values is discussed. $Co_3O_4$ samples with the highest surface area values were tested in the CO oxidation.

(Received November 14, 2006; accepted April 12, 2007)

*Keywords:* $Co_3O_4$, CO oxidation, Precipitation method, Nanopowders

## 1. Introduction

Tricobalt tetraoxide, $Co_3O_4$, with spinel structure has been studied for its wide range of applications including catalyst for CO oxidation [1-4], reduction of NO with propane or propene in oxygen excess when it is supported on alumina, silica or zirconia [5], *p*H sensor [6] and electrode material for lithium ion batteries [7].

Many efforts have been focused to prepare nanocrystalline $Co_3O_4$ with narrow size distribution and high surface area values by different methods as homogeneous precipitation [8], polymer combustion [9], sol-gel route [10], decomposition of cobalt salts [7,11] or complex salts [12,13], inverse microemulsion method [14], hydrothermal oxidation [15].

J. Jansson et al. [4] have investigated the low temperature CO oxidation over cobalt oxide catalysts. CO deactivates the oxidised catalysts, but the rate of deactivation can be suppressed by having a high $O_2$/CO ratio. In the mechanism proposed by Jansson *et al.*, CO adsorbs on octahedral coordinated surface $Co^{3+}$ ions.

(1) The adsorbed CO reacts with activated oxygen, already present on the cobalt oxide surface and desorbs as $CO_2$.

(2) The reduced cobalt is deoxidized by gas phase oxygen or it is further reduced by CO thus deactivating the site.

(3) $CO_2$ can adsorb on the surface and form surface carbonate species.

An $^{18}O$-isotope study showed that oxygen participating in the oxidation of CO comes from oxygen bound to the cobalt oxide surface. Presence of water and/or hydrocarbons seems to poison the activity cobalt oxide catalyst [16]. J. Jansson et al. [1] have explained the deactivation of $Co_3O_4$ in the CO oxidation by a surface reconstruction of the cobalt oxide making the cobalt ions inactive for CO adsorption. It is known that in $Co_3O_4$, $Co^{3+}$ ions are originally in the octahedral position and $Co^{2+}$ in tetrahedral positions. During the CO oxidation reaction, surface reconstruction occurs where active octahedral coordinated $Co^{3+}$ ions are transformed to tetrahedral coordinated $Co^{3+}$ without any change in cobalt ions oxidation state. On the base of in situ FT-IR studies, H.K. Lin et al. [4] have suggested that CO and $O_2$ are co-adsorbed over $Co_3O_4$. The oxygen of lattice is more active than $O_2$ adsorbed which could oxidise CO to produce $CO_2$.

From TPR study it is known that the reduction of bulk $Co_3O_4$ does not start until 573K and the temperature of the beginning $Co_3O_4$ reduction increases with the increasing of temperature preparation and the crystal size of $Co_3O_4$. It can be expected that the samples with spherical particles obtained at lower temperature have more structural defects than the well-crystallised polyhedral ones obtained at higher temperatures. These defects at the surface should facilitate the reduction [17].

This paper deals with the synthesis of $Co_3O_4$ nanopowders with large surface area values by precipitation at constant *p*H. We report the catalytic activities of some $Co_3O_4$ samples for CO oxidation to $CO_2$.

## 2. Experimental

*Samples preparation.* For obtaining $Co_3O_4$ powders, two cobalt salts and ammonia or potassium hydroxide as precipitating agent have been used. For the preparation of sample $A_1$, 0.1M $Co(NO_3)_2$ (Alpha Aesar) solution and 0.2 M $NH_3$ solution as precipitation agent were added together to 150 mL water at constant *p*H (*p*H=9), at room temperature. The green precipitate was filtrated, washed and dried at 110°C overnight and then calcined in air in different conditions (variable temperature and time). For samples $A_2$ and $A_4$ preparation, 0.5M $Co(NO_3)_2$ solution and 0.2M $NH_3$ and KOH solution respectively, as precipitation agent were drop wised to 150 mL water at constant *p*H (*p*H=9), at room temperature. Then the reaction mixture was kept at 80°C for 4h. The precipitate

colour turned from green to black. Then the precipitate was centrifuged, washed, dried at 110°C overnight and then calcined at 200°C for 4h, in air. The sample $A_3$ has been prepared as the sample $A_2$, but using 0.1M cobalt nitrate solution. The dried precipitate was calcined in different conditions, at 200°C for 4h or 8h and 300°C for 4h. The sample $A_5$ was obtained from 0.5M $CoSO_4$ (Alpha Aesar) solution and 0.2 M $NH_3$ solution as precipitating agent at *p*H=9.5. The precipitation was performed at room temperature and then the reaction mixture was kept at 80°C for 4h under stirring. The precipitate colour turned from blue to green. The precipitate was filtered, washed until there were no sulphate ions presented in the solution and then dried at 110°C overnight. The calcination of the precipitate was performed at variable temperature and time.

*Samples characterisation*. The samples were characterised by X-ray diffraction (XRD), transmission electron microscopy (TEM) and specific surface area measurements (BET method). For establish the condition of thermal treatment of precipitates for obtaining pure spinel phase of $Co_3O_4$, the samples before calcination were investigated by differential thermal analysis - thermogravimetric analysis (DTA-TG). Thermal analysis was carried out in air, in 20°-600°C temperature range with a heating rate of 5°C /min using a Setaram TG-DTA 92 equipment. X-ray diffraction patterns were obtained using a Bruker D5005 with $CuK_\alpha$ radiation at a step of $0.02^o$/s in the range $2\theta = 3$ to $80^o$. Transmission electron micrographs were obtained using a JEOL 2010 electron transmission microscope.

*Catalytic tests*. Activity tests of $Co_3O_4$ samples for CO oxidation reaction were carried out at atmospheric pressure, in a fix bed reactor with 10 mm diameter which contained 0.5 g of catalyst powder. The reactor was heated in a furnace connected to a temperature controller. The total flow rate of reactant mixture (2.4% CO, 2% $O_2$ balanced with He) was 50 $cm^3min^{-1}$ STP (standard temperature and pressure). The flows of CO (19.89% CO diluted with He), $O_2$ and He were controlled by separate thermal mass flow controllers. The corresponding gas hour space velocity (SV) of reactant mixture was 3000 $cm^3\ h^{-1}$/g catalyst or 6000 $cm^3\ h^{-1}$/g catalyst. In all experiments the catalysts were first pretreated in 2% or 10% $O_2$ balanced with He at 150 °C for 2h or 300 °C for 0.5h and cooled at room temperature in the mixture of gases. The analysis of the effluent gas was performed by gas chromatography (Varian CP 2003 Micro GC) equipped with a TCD detector. The reaction products were analysed by using a Poraplot Q column for $CO_2$ and a 5Å molecular sieve column for CO and $O_2$. The heating rate of the catalysts up to the temperature when the conversion of CO is 100% was $1°\ min^{-1}$.

## 3. Results and discussion

The $Co_3O_4$ samples were characterised by XRD, thermal analysis (DTA-TG), transmission electronic microscopy and BET surface area measurements. The crystallite size values were calculated by means of the Scherrer's equation, $D = K\lambda/\beta\cos\theta$, where K is a constant equal to 0.9, $\lambda$, the wavelength of the X-ray used, $\beta$, the full width at half-maximum (FWHM) of the (311) diffraction peak ($2\theta = 36.45°$). Table 1 summarises some properties of the cobalt oxide samples as function of the synthesis parameters.

*Table 1. Physico-chemical characterisation of the prepared cobalt oxide samples.*

| *Sample* | *Preparation conditions* | *Thermal treatment* | *Nature of phases and crystallite size [nm]* | *S [$m^2$/g]* |
|---|---|---|---|---|
| **$A_1$** | pH=9, T=25°C 0.1M $Co(NO_3)_2$ 0.2M $NH_3$ | 400°C, 4h | $Co_3O_4$, 22 | 26.78 |
| | | 300°C, 4h | $Co_3O_4$, 15 | 71.44* |
| | | 400°C, 2h | $Co_3O_4$, 18 | 38.61 |
| **$A_2$** | pH=9, T=80°C, 4h 0.5M $Co(NO_3)_2$ 0.2M $NH_3$ | Drying at 110°C | $Co_3O_4$, 16 | 106.78* |
| | | 200°C, 4h | $Co_3O_4$, 20 | 93.46 |
| **$A_3$** | pH=9, T=80°C, 4h 0.1M $Co(NO_3)_2$; 0.2M $NH_3$ | 200°C, 4h | $Co_3O_4$+ CoO(OH) | - |
| | | 200°C, 8h | $Co_3O_4$+ CoO(OH) | - |
| | | 300°C, 4h | $Co_3O_4$, 28 | 32.47 |
| **$A_4$** | pH=9, T=80°C, 4h 0.5M $Co(NO_3)_2$ 0.2M KOH | 200°C, 4h | $Co_3O_4$, 28 | 71.13 |
| **$A_5$** | pH=9.5 0.5M $CoSO_4$ 0.2M $NH_3$; T=80°C, 4h | 400°C, 8h | $Co_3O_4$+ impurity, 8 nm | - |
| | | 500°C, 4h | $Co_3O_4$+impurity 9 nm | - |

*Samples tested for CO oxidation

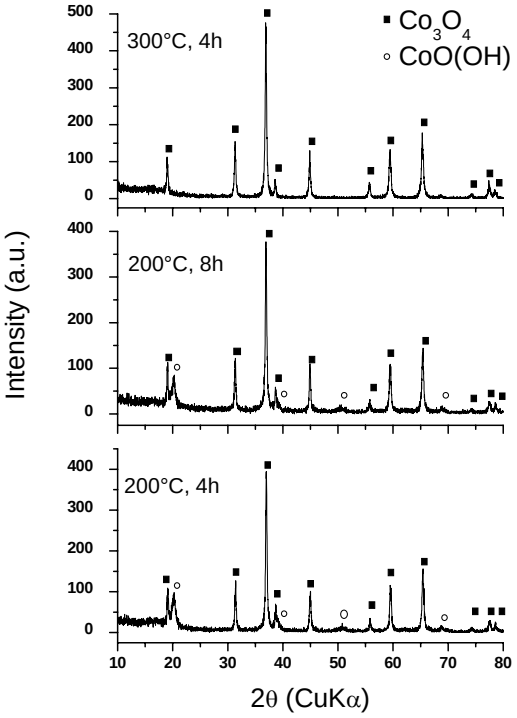


*Fig. 1. XRD patterns of the sample $A_3$ obtained by different thermal treatments.*

The sample $A_1$, calcined at 300°C for 4h has the cubic spinel structure of $Co_3O_4$ with lattice parameter, $a$=8.0614 Å and 15 nm crystallite size. The particle size increases with temperature and with time of thermal treatment. The crystallite size and the specific surface area values of $Co_3O_4$ samples determined by BET method are listed in Table 1. By changing the temperature of precipitation and by varying the $Co(NO_3)_2$ concentration, it was possible to change the composition of the final material. If the cobalt hydroxide obtained by precipitating of cobalt nitrate is heated at 80°C for 4h with stirring in the reaction medium, the $Co^{2+}$ ions are oxidised in aqueous medium to $Co^{3+}$ and a mixture of $Co_3O_4$ and CoO(OH) ($A_3$) and $Co_3O_4$ single phase is obtained at 200°C ($A_2$).

For sample $A_3$ it can notice that the only $Co_3O_4$ phase with the spinel structure is formed at 300°C while for $A_2$ or $A_4$, $Co_3O_4$ phase is formed at 200°C (Figs. 1, 2). More diluted solution of cobalt nitrate imposed an increase of the calcination temperature in order to obtain $Co_3O_4$ from CoO(OH) (Fig. 2).

The sample $A_4$ calcined at 200°C, 4h is single phase with cubic spinel structure with lattice parameter $a$=8.0877 Å. Using as precipitating agent, potassium hydroxide solution instead of $NH_3$ with the same concentration, 0.5M $Co(NO_3)_2$, bigger crystallite size and smaller specific surface area value is observed for $Co_3O_4$ (Table 1). If the cobalt hydroxide is obtained by precipitating of cobalt sulphate, $Co_3O_4$ is obtained at higher temperature and the particle size is smaller (sample $A_5$, Table 1).

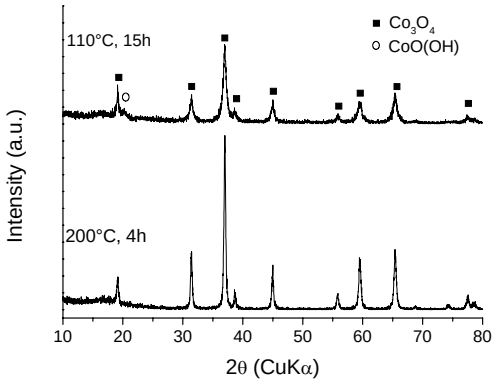


*Fig. 2. XRD patterns of the sample $A_2$ dried at 110°C and calcined in air at 200°C for 4h.*

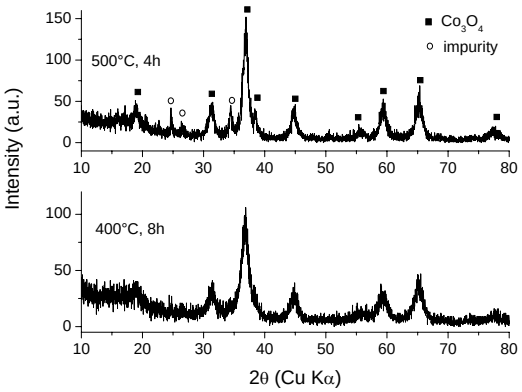


*Fig. 3. XRD patterns for the sample $A_5$.*

When cobalt sulphate has been used, $Co_3O_4$ is formed at higher temperature and it is not well crystallised. The XRD patterns revealed the presence of an impurity that could be from cobalt sulphate (Fig. 3). Unlike the samples $A_2$ or $A_4$, the precursor of the sample $A_5$, before the calcination is amorphous.

The DTA curve of the sample $A_1$ (Fig. 4) presents two endothermic effects at 177°-220°C and a big one at 220°-290°C ($T_{max}$=255°C) temperature range that could be assigned to decomposition of cobalt oxyhydroxyde, CoO(OH) and $Co_3O_4$ formation. The experimental total weight loss is 6%. The DTA curve of sample $A_5$ (Fig. 5) presents an endothermic peak at 108°C assigned to the water loss, an exothermic effect at 173°C and two endothermic effects at 225°C and at 236°-350°C temperature range. The first two effects are partial overlapped. The total experimental weight loss is 16.4%. The DTA-TG curve for the sample $A_5$ is similar with DTA-TG curve of the sample $A_1$, but the endothermic effects assigned with decomposition of CoO(OH) are shifted toward higher temperature than for sample $A_1$.

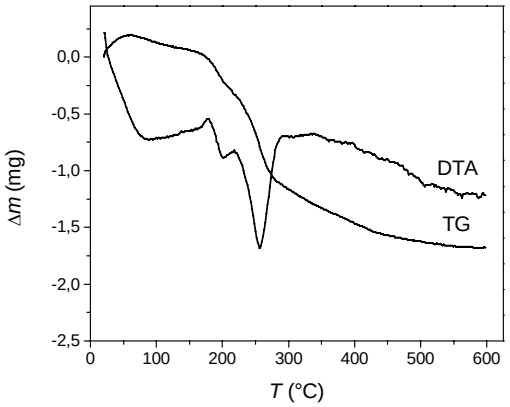


*Fig. 4. DTA-TG analysis of the $A_1$ sample.*

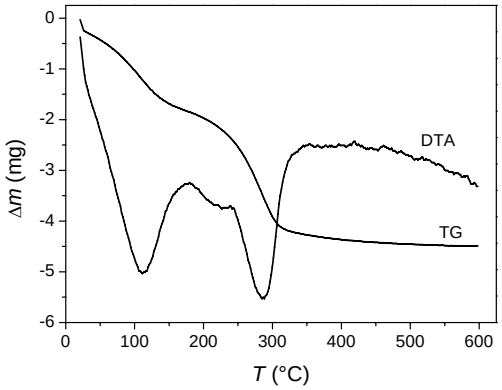


*Fig. 5. DTA-TG analysis of the $A_5$ sample.*

TEM pictures show that $Co_3O_4$ sample named $A_1$, calcined at 300 °C for 4h presents spherical particles with 12-15 nm diameter (Fig. 6). TEM investigation of $A_2$ sample (Fig. 7) obtained at 200 °C – 4h shows that the oxide presents some agglomeration of spherical particles with air channels and higher porosity.

The $Co_3O_4$ samples with high surface area values have been tested in the CO oxidation to $CO_2$, marked with "*" in the Table 1. The two samples tested for CO oxidation have similar activities. Fig. 8 shows the temperature dependence of CO conversion in two stages of heating - cooling for $Co_3O_4$ ($A_2$); one stage, after a pretreatment at 150 °C for 5h and the other, after the catalyst was kept in the reaction mixture overnight. Based on catalytic data we could notice that the activity of $Co_3O_4$ is influenced by the conditions of the pretreatment, especially by the temperature of it. Higher activities for the sample pretreated at 300 °C were obtained. It can notice that the concentration of oxygen in the mixture of the gases used for the pretreatment has small influence on the catalytic activity of $Co_3O_4$ (Fig. 9).

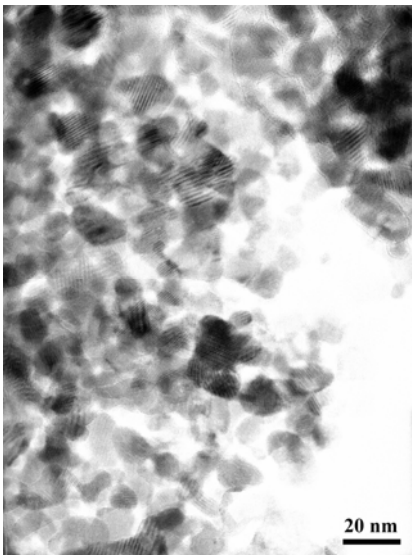


*Fig. 6. TEM picture of the sample $A_1$.*


*Fig. 7. TEM picture of the sample $A_2$.*

The difference between the temperature of 100% conversion of CO ($T_{100}$) when the catalyst was pretreated at 300 °C is more than 100 °C. For example, after a pretreatment at 300 °C, the total conversion of CO was obtained at room temperature in comparison with 141°C for the catalyst pretreated at 150 °C. From Fig. 10, it can notice that $Co_3O_4$ looses the activity in time, it is active 300 min. In all the catalytic tests it noticed that the catalytic activity of $Co_3O_4$ is higher in the cooling stage than in the heating stage. The difference between the activity in the two stages is smaller when the concentration of CO in the mixture of feed gas is smaller (Fig. 11).

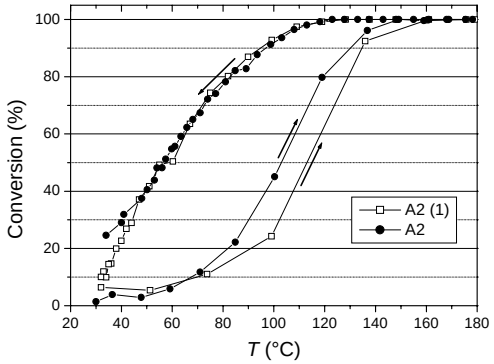


*Fig. 8. Catalytic activity of the sample $A_2$ at SV of 3000 $cm^3$ $h^{-1}$/ g: (1) pretreatment at 150°C, 2h in 2% $O_2$.*

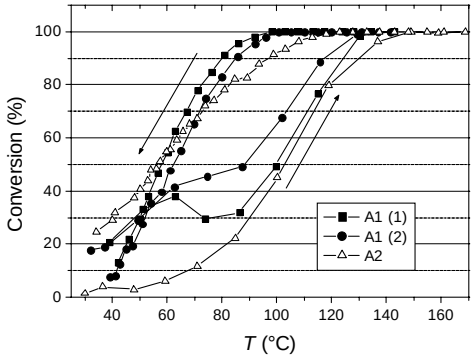


*Fig. 9. Catalytic activity of $Co_3O_4$ samples at a SV of 3000 $cm^3$ $h^{-1}$/ g : (1) pretreatment at 150°C, 2h in 2% $O_2$; (2) pretreatment at 150°C, 2h in 10% $O_2$.*

There are two surface oxygen ions, one is bonded to one Co(II) ion and one Co(III) ion, while the second surface oxygen has three Co(III) ions as nearest neighbours. Based on density functional theory it is known that the oxygen vacancy resulted from the removing of the former superficial oxygen is more reluctant to oxidise than the later one [18]. It could explain the higher activity of $Co_3O_4$ in the cooling stage by changing of the concentration of defects, more exactly the concentration of the type of oxygen vacancies.

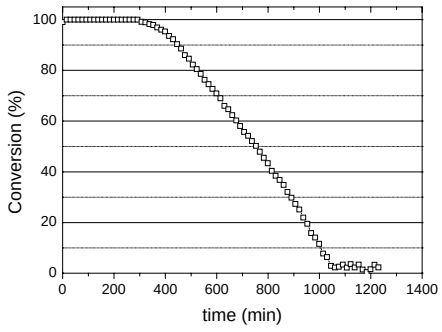


*Fig. 10. The CO conversion to $CO_2$ in time on $A_1$ sample at a SV of 3000 $cm^3$ $h^{-1}$/ g pretreated at 300°C, 0.5h in 10% $O_2$.*

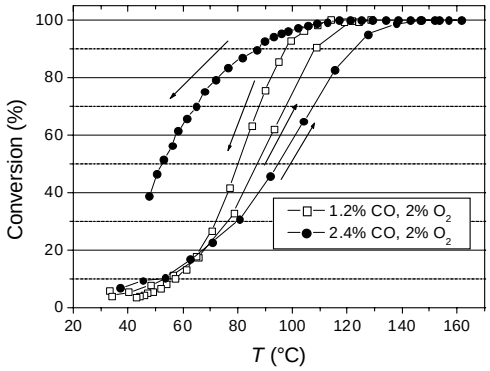


*Fig. 11. The CO conversion to $CO_2$ function of the reaction temperature on sample $A_1$ at SV of 6000 $cm^3$ $h^{-1}$/ g: pretreated at 300°C, 0.5h in 10% $O_2$.*

## 4. Conclusions

$Co_3O_4$ nanopowders with high surface area were prepared by homogeneous precipitation and then tested for CO oxidation. Based on catalytic data it could conclude that the activity of $Co_3O_4$ is influenced by the pretreatment conditions, especially by the temperature of it. The catalytic activity for CO total oxidation of $Co_3O_4$ is higher in the cooling stage than in the heating stage and this difference is higher when the concentration of CO in the inlet gas is bigger.

**Acknowledgements**

The authors acknowledge Dr. M. Aouine for his help in obtaining the TEM results.

## References

[1] J. Jansson, A. E. C. Palmqvist, E. Fridell, M. Skoglundh, L. Osterlund, P. Thormahlen, V. Langer, J. Catal. **211,** 387 (2002).
[2] C. B. Wang, C. W. Tang, H. S. Tsai, S. H. Chien, Catal. Lett. **107**, 223 (2006).
[3] H. K. Lin, C. B. Wang, H. C. Chiu, S. H. Chien, Catal. Lett. **86,** 63 (2003).
[4] J. Jansson, M. Skoglundh, E. Fridell, P. Thormahlen, Top. Catal. **16/17,** 385 (2001).
[5] L. F. Liotta, G. Pantaleo, A. Macaluso, G. Di Carlo, G. Deganello, Appl. Catal. A: General, **245**, 167 (2003).
[6] L. Qingwen, L. Guoan, S. Youqin, Anal. Chim. Acta, **409,** 137 (2000).
[7] Z. Yuan, F. Huang, C. Feng, J. Sun, Y. Zhou, Mater. Chem. Phys. **79,** 1 (2003).
[8] M. M. Natile, A. Glisenti, Chem. Mater. **14**, 3090 (2002).
[9] J. Jiu, Y. Ge, X. Li, L. Nie, Mater. Lett. **54**, 260 (2002).

[10] F. Svegl, B. Orel, I. Grabec-Svegl, V. Kaucic, Electrochim. Acta **45**, 4359 (2000).
[11] S. Ardizzone, G. Spinolo, S. Trasatti, Electrochimica Acta, **40,** 2683 (1995).
[12] G. Furlanetto, L. Formaro, J. Colloid Interface Sci. **170,** 169 (1995).
[13] M. Sato, H. Hara, H. Kuritani, T. Nishide, Sol. Energy Mater. Sol. Cells **45**, 43 (1997).
[14] Y. Liu, G. Wang, C. Xu, W. Wang, Chem. Commun. 1486 (2002).
[15] Y. Jiang, Y. Wu, B. Xie, Y. Qian, Mater. Chem. Phys. **74**, 234 (2002).
[16] P. Thormahlen, M. Skoglundh, E. Fridell, B. Andersson, J. Catal. **188**, 300 (1999).
[17] D. Potoczna-Petru, L. Kepinski, Catal. Lett., **73**, 41 (2001).
[18] P. Broqvist, I. Panas, H. Persson, J. Catal. **210**, 198 (2002).

*Corresponding author: danaberger01@yahoo.com